Climate-Related Variation of the Human Nasal Cavity

Marlijn L. Noback,[1,2]* Katerina Harvati,[1] and Fred Spoor[2,3]

[1]*Paleoanthropology Section, Senckenberg Center for Human Evolution and Paleoecology, Eberhard Karls Universität Tübingen, Department of Early Prehistory and Quaternary Ecology, 72070, Tübingen, Germany*
[2]*Department of Cell and Developmental Biology, University College London, London, WC1E 6JJ, United Kingdom*
[3]*Department of Human Evolution, Max Planck Institute for Evolutionary Anthropology, 04103 Leipzig, Germany*

KEY WORDS nose; adaptation; geometric morphometrics; PLS

ABSTRACT The nasal cavity is essential for humidifying and warming the air before it reaches the sensitive lungs. Because humans inhabit environments that can be seen as extreme from the perspective of respiratory function, nasal cavity shape is expected to show climatic adaptation. This study examines the relationship between modern human variation in the morphology of the nasal cavity and the climatic factors of temperature and vapor pressure, and tests the hypothesis that within increasingly demanding environments (colder and drier), nasal cavities will show features that enhance turbulence and air-wall contact to improve conditioning of the air. We use three-dimensional geometric morphometrics methods and multivariate statistics to model and analyze the shape of the bony nasal cavity of 10 modern human population samples from five climatic groups. We report significant correlations between nasal cavity shape and climatic variables of both temperature and humidity. Variation in nasal cavity shape is correlated with a cline from cold–dry climates to hot–humid climates, with a separate temperature and vapor pressure effect. The bony nasal cavity appears mostly associated with temperature, and the nasopharynx with humidity. The observed climate-related shape changes are functionally consistent with an increase in contact between air and mucosal tissue in cold–dry climates through greater turbulence during inspiration and a higher surface-to-volume ratio in the upper nasal cavity. Am J Phys Anthropol 000:000–000, 2011.

As humans live and breathe in a wide range of environments, including those which can be seen as "extreme" from a perspective of respiratory function (Baker, 1988), the nasal cavity has long been hypothesized to play an important role in climatic adaptation. Because the lungs are very sensitive to air temperature and humidity, it is important that the nose regulates these particular factors (Negus, 1958; Cole, 1982). The nasal cavity (see Fig. 1) is essential for conditioning the air because this is where exchange of heat and moisture mostly occur (Franciscus and Long, 1991). Research linking modern human nasal morphology with climate, however, has focused mainly on the outer nose and the nasal aperture (Thomas and Buxton, 1923; Davies, 1932; Weiner, 1954; Carey and Steegmann, 1981; Franciscus and Long, 1991; Roseman, 2004; Hubbe et al., 2009). None of the external measurements deals with the morphology of the nasal cavity behind the nasal aperture, e.g., the amount of turbinate area or the depth of the cavity (St. Hoyme and Iscan, 1989), even though this is the part of the nose most crucial for conditioning the air (Franciscus and Long, 1991; Yokley, 2009).

Research on the relationship between climate and the nasal cavity itself has been limited, largely because of the difficulties involved in measuring this complicated internal structure (Yokley, 2009), with only a small number of studies addressing this topic. Morgan et al. (1995) reported differences in the size of the cross-section area of the nasal cavity between sub-Saharan Africans and European and Asian groups. Corey et al. (1998) studied the nasal volume in different geographic groups, but did not find significant differences. More recent work by Yokley (2009) found significant differences in the nasal cavity surface/volume ratio between European and African Americans in an (artificially) decongested condition. These studies are limited by the use of linear measurements, which cannot fully address the three-dimensional properties of the nasal cavity, as well as by their general treatment of climatic factors, which are considered only in broad terms.

This work aims to fill this gap by assessing the relationship between climate and nasal cavity shape using three-dimensional geometric morphometric methodology and climate data representing temperature and vapor pressure, and taking into account the diverse functional demands on nasal cavity shape.

BACKGROUND

Nasal cavity shape and function

Nasal cavity morphology is the most important factor in determining the stream mechanics of nasal air flow (Mlynski et al., 2001). The nasal cavity can be divided

Grant sponsor: Huygens Scholarship Programme—Talentprogramme; Grant number: HSP-TP.07/192.

*Correspondence to: Marlijn Noback, Eberhard Karls Universität Tübingen, Department of Early Prehistory and Quaternary Ecology, Rümelinstrasse 23, 72070 Tübingen, Germany. E-mail: marlijn.noback@ifu.uni-tuebingen.de

Received 16 November 2010; accepted 31 January 2011

DOI 10.1002/ajpa.21523
Published online in Wiley Online Library (wileyonlinelibrary.com).

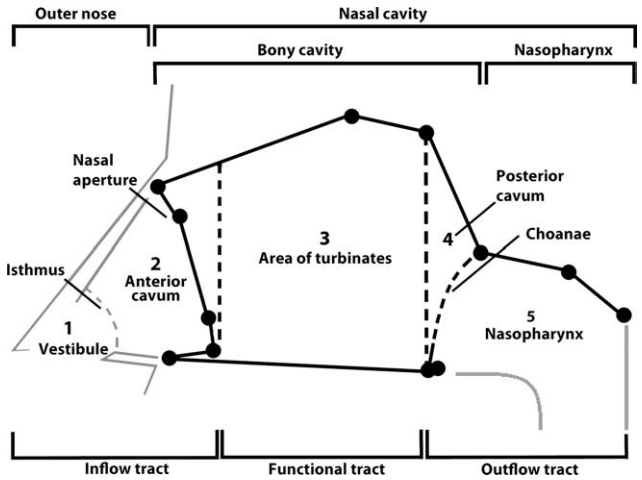

Fig. 1. Structural elements of the nose in inspiratory direction (adapted from Mlynski et al., 2001). The black lines indicate the nasal cavity model used in this study (see Fig. 3). In inspiration direction, the vestibule (1) changes the direction of the air. The concave isthmus makes the airflow diverge. Depending on the shape of the anterior cavum (2) and the flow velocity, airflow changes from laminar flow to turbulent flow in the anterior or posterior part of the turbinate area (3). The posterior cavum (4) decreases the amount of turbulence and forces the air through the convex choanae that cause the air streamlines to converge. The laminar flow that results flows through the nasopharynx (5) where it changes direction into the lower respiratory tract (Mlynski et al., 2001).

into three different functional regions that influence the airflow: 1) an inflow area (vestibule, isthmus and anterior cavum), 2) a functional area (area of the turbinates), and 3) an outflow area (posterior cavum, choanae, and nasopharynx) (Mlynski et al., 2001; see Fig. 1). Because the relative dimensions and properties of the nasal cavity directly affect air flow during both inspiration and expiration, variation in nasal cavity morphology directly impacts its function.

One of the most important functions of the nasal cavity is to condition inspired air so as to prevent damage of the sensitive mucosal tissues of the lungs, where the air must be at body temperature and nearly saturated to facilitate gas exchange (Negus, 1958). Besides warming and humidifying the inspired air, moisture retention during expiration is also a crucial function of the external nose and nasal cavity, especially in dry environments (Franciscus and Trinkaus, 1988). Conflicting statements have been made regarding the function of the nose and nasal cavity in thermoregulation: (selective) cooling (Davies, 1932; Cabanac and Caputa, 1979; Dean, 1988; Mariak et al., 1999), prevention of heat loss (Negus, 1958), or no evidence for such function at all (Deklunder et al. 1991; Jessen and Kuhnen, 1992; Mekjavic et al., 2002; Maloney et al., 2007). The human nose lacks the specialized carotid rete present for the cooling purpose in some animals; the surface of the nose is particularly small compared with that of the body, making its influence on body temperature rather small (Weiner, 1954), and mouth breathing appears to be more effective to cool down (Negus, 1958; Lieberman, 2011). With respect to selective brain cooling involving nasal breathing recent experimental studies found no evidence that this form of thermoregulation exists at all in humans and other primates (Mekjavic et al., 2002; Maloney et al., 2007). Hence, in this study we focus explicitly on the function of the nasal cavity in conditioning the air on inspiration and retaining moisture on expiration.

Table 1 gives an overview of the demands that different climate types pose on the nose in terms of the level of air-conditioning that is needed, both during inspiration and expiration.

As breathing in hot and humid environments requires almost no warming or humidifying of the incoming air, we regard this type of environment as least stressful in terms of air-conditioning to maintain lung function. The temperate regions show temperature and humidity values between those of hot and humid and cold and dry environments, and are therefore regarded as being intermediately stressful for breathing.

Warming and humidifying inspired air is influenced by the amount of contact between nasal mucosal tissue and the air (Mowbray and Gannon, 2001; Clement and Gordts, 2005). Several important features of the nasal cavity enhance this contact, including 1) greater surface-volume ratio, 2) increased residence time, and 3) greater turbulence (Churchill et al., 2004; Clement and Gordts, 2005).

Greater surface-volume ratio. Increasing the mucosal contact surface per unit of air volume that is inspired, enhances the exchange of moisture and warmth between the air and the mucosal tissue. The surface-volume ratio can be increased by an elaborate turbinate system, by an increase in length of the cavity and by a smaller cross-sectional area (narrowing) of the nasal cavity. A nasal cavity that is too narrow, on the other hand, increases nasal resistance and flow velocity, which in turn decrease temperature and humidity exchange with the nasal wall (Inthavong et al., 2007). There is therefore a limit to decreasing the nasal cross-sectional area for enhancing air-conditioning.

Residence time. To improve air-conditioning in narrow nasal cavities, an increase of the time the air is inside the nasal cavity (residence time) becomes important (Inthavong et al., 2007). It is expected that relative lengthening of the nasal cavity provides this increase of residence time.

Turbulence. For air-conditioning to be efficient, turbulence is necessary (Cole, 2000; Clement and Gordts, 2005). The higher the degree of turbulence, the better the incoming air gets mixed within the boundary layer of the nasal walls and mucus, thus directly influencing the efficiency of moisture and heat exchange during respiration (Franciscus and Long, 1991; Cole, 2000; Churchill et al., 2004). Especially in the posterior part of the turbinate chamber, turbulence is essential for convective heat transfer (Inthavong et al., 2007). Turbulence increases with increased diameter (i.e., breadth and/or height) of the tube (Churchill et al., 2004) and with greater shape irregularity of the tube (Courtiss and Goldwyn, 1983). Another turbulence inducing factor is the relative increase in cross-sectional area (a pronounced diameter size step) between the nasal aperture and the turbinate chamber during inspiration, and between the choana and the turbinate chamber during expiration, relative to the anteroposterior length of the anterior and posterior cavum, respectively (see Fig. 1; Mlynski et al., 2001). The smaller the opening through which air has to flow relative to the size of the turbinate chamber, and the shorter the distance that it has to travel to enter this chamber, the greater the turbulence.

TABLE 1. Overview of air-conditioning demands in different climate types

Climate	Humidity adjustment of air	Temperature adjustment of air	Expected stress level
Cold–dry	Much humidification needed. Moisture conservation during expiration	Much warming needed. Minimization of heat loss during expiration	Very high
Cold–humid	Much humidification needed. Cold air contains little moisture. Moisture conservation during expiration	Warming of air needed. Minimization of heat loss during expiration	High
Temperate	Seasonal fluctuations in humidity, but never extreme	Seasonal fluctuations in temperature, but never extreme	Intermediate
Hot–dry	Humidification needed: hot dry air can extract moisture from the body. Moisture conservation during expiration	Air temperature can be higher than body temperature. Cooling rather than heat preservation	Medium
Hot–humid	No air-conditioning needed	No air-conditioning needed. Cooling rather than heat preservation	Low

Other features, not measured in this study, such as greater airflow velocity (Clement and Gordts, 2005), downward facing nares and/or large turbinates also influence airflow turbulence (Churchill et al., 2004).

It is important to point out that the nasal cavity shape requirements to enhance one or the other of the above properties are sometimes contradictory, e.g., turbulence is enhanced by a wider cavity, whereas a narrow cavity increases the surface to volume ratio. With so many different functional processes at work, the nasal cavity will likely show a compromise morphology (Churchill et al., 2004).

Hypotheses

This research aims to investigate a possible functional relationship between nasal cavity morphology and climate, by examining the following two hypotheses and their predictions:

1. Climate affects nasal morphology.
   - a There are significant correlations between nasal cavity shape and climatic factors of temperature and vapor pressure.
   - b Trends in nasal cavity shape will follow a climatic trend from least to most physiologically demanding environments for breathing: from hot–humid to cold–dry.
   - c Nasal morphology is related to climate irrespective of nasal cavity size.

2. Cold–dry climates, most demanding in terms of breathing, have resulted in nasal cavity morphology which enhances conditioning of the air. Cold–dry groups will show air-wall contact enhancing features:
   - a decrease in relative breadth and/or height to increase surface/volume ratio.
   - b increased relative length of the cavity to increase residence time.
   - c increased turbulence through larger breadth and especially relative height of the cavity, and through a pronounced relative diameter size step between the cross-sectional area of the anterior cavum and the turbinate chamber, and between the posterior cavum and the turbinate chamber.

MATERIALS AND METHODS

Samples

The 100 crania from 10 populations were selected from collections housed in the Natural History Museum London and the American Museum of Natural History. The samples come from five zones of diverse climatic stress (Beals et al., 1984), and attempt to represent indigenous populations of each area, not dominantly affected by modern western lifestyle and health care. Table 2 summarizes population location, sample size, and the collections where the cranial material are housed, climate zone, temperature, and vapor pressure data. MN measured the listed material from the Natural History Museum in London; FS measured the listed material from the American Museum of Natural History in New York. In an attempt to separate genetic relatedness from climatic type as a possible influence on nasal morphology, at least two populations from different continents were selected for each climate zone.

Selection of crania was based on the presence of all features where the landmarks were taken. Only adult crania were included, based on fusion of the sphenooccipital synchondrosis. Individuals with substantial *in vivo* tooth loss or signs of other dental pathologies were excluded, as such conditions may influence palatal morphology and thus the nasal floor. Attempts to obtain samples with equal numbers of males and females were not successful. The number of available specimens per population was severely hampered by the difficulty to find skulls sufficiently preserved to measure all landmarks, and few have reliable historical gender information. We chose not to estimate sex from cranial morphology because established sex estimation methods are partly based on robustness, including the nasal area, and thus might result in biased samples and results. Corey et al. (1998) and Franciscus (1995) showed that indigenous men and women from the same geographical area show no significant difference in nasal morphology, and any major climate-related trend can be expected to affect both sexes following a similar pattern (Hall, 2005), especially, since it is predominantly shape, rather than size that is analyzed here.

Climate data of temperature and vapor pressure (Table 2) were obtained using the KNMI Climate Explorer compiled by Dr G. J. van Oldenborgh (http://climexp.knmi.nl; Oldenborgh et al., 2005), retrieving monthly observations from the CRU TS3 database at 0.5 degree, for the years 1901–2006. Although this dataset likely does not fully reflect the climatic conditions of the

TABLE 2. Overview of populations, number of individuals per population per collection (AMNH = American Museum of Natural History, measured by FS; NHM = Natural History Museum London, measured by MN), and climatic data per population. Temperature (T) in degrees Celsius, vapor pressure (VP) in hectopascal

	Collection (#)	Tmean	Tmin	Tmax	VPmean	VPMin	VPmax
Cold and dry							
Greenland	NHM(9), AMNH(1)	−5.69	−16.88	6.28	3.90	1.48	7.73
Indian Point Siberia	AMNH(10)	−5.11	−16.86	7.82	3.80	1.11	8.02
Cold and humid							
Aleutian Islands	AMNH(10)	3.52	−1.18	9.69	6.89	4.26	11.04
Tierra del Fuego and Patagonia	NHM(7), AMNH(2)	4.97	0.98	8.73	6.13	4.97	7.56
Temperate							
Central Europe	NHM(11)	10.29	−1.14	20.62	10.19	4.81	16.48
Chatham Islands	NHM(10)	12.51	7.74	18.11	19.76	16.44	22.88
Hot and dry							
South Africa	NHM(9), AMNH(1)	17.39	10.55	23.20	11.03	7.07	15.51
Western Australia	NHM(8), AMNH(2)	21.58	14.13	28.14	12.67	9.12	17.19
Hot and humid							
Gabon	NHM(10)	24.95	23.00	26.05	25.74	22.95	27.05
Papua New Guinea	AMNH(10)	25.52	24.32	26.41	25.22	22.94	26.66

TABLE 3. Definitions of the 21 nasal cavity landmarks and description of the landmarks representing the air-wall contact features used in this study

Landmark	Osteometric name	Description	Type
1,3	–	Anterior edge of anterior ethmoid foramen.	2
2,4	–	Posterior edge of posterior ethmoid foramen.	2
5	Rhinion	Midline point at inferior free end of the internasal suture.	1
6,7	–	Nasomaxillary suture at piriform aperture.	1
8,9	Alare	The lateralmost margin of nasal aperture.	1
10,11	–	Inferiormost margin of nasal aperture.	2
12	ANS	Anterior nasal spine: tip of the median bony process of the maxilla.	2
13	PNS	Posterior nasal spine: posterior tip of midsagittal bony palate.	2
14,15	–	Inferolateral choanal corner.	2
16,17	–	Superiormost margin of choana.	2
18	Hormion	Most posterior midline point on the vomer.	1
19,20	–	Posterosuperior end of medial pterygoid plate.	2
21	–	Most inferior midpoint on the pharyngeal tubercle.	3

past thousands of years, during which time the differentiation of the modern human groups examined took place, it is among the most exhaustive and detailed climatic databases currently available. The data were obtained for the geographical location of each individual cranium, but when no exact provenance is known an area rather than single location was used to represent the region of origin of that specimen. For each specimen the following values were calculated: mean yearly temperature (Tmean), coldest monthly temperature (Tmin), warmest monthly temperature (Tmax), mean yearly vapor pressure (VPmean), lowest monthly vapor pressure (VPmin), and highest monthly vapor pressure (VPmax). Subsequently, sample means of the six variables were calculated for each of the 10 populations.

Measurements

Data were collected with a Microscribe 3DX portable digitizer in the form of three-dimensional coordinates of 21 nasal cavity landmarks. Microscribe digitization is limited to externally accessible landmarks. We therefore chose our landmarks as to best reflect the major aspects of nasal cavity shape that affect air-wall contact and hence conditioning of inspired air (Table 3, Figs. 2 and 3). Some of these are well-established anthropological landmarks (Bräuer, 1988), whereas others were specifically defined to quantify particular aspects of the nasal cavity. In addition to type 1 landmarks, it was necessary to include several type 2 (8) and type 3 (1) landmarks to accurately describe the nasal cavity (Bookstein, 1991).

To better visualize the complex shape represented by our landmark set we constructed a wireframe model using MorphoJ (version 1.01c, Klingenberg, 2011) which makes it easier to visualize and interpret the landmark configuration. Figure 1 shows the terminology used to describe different parts of the nasal cavity model (modified from Mlynski et al., 2001). As the bony part of the nasal cavity and the nasopharynx form one functional complex, both are included in the term "nasal cavity." This term excludes the external, fleshy part of the nose (the outer nose). We used relative distances between landmarks (see Fig. 3) to describe elements of the nasal cavity that influence air-wall contact. Changes in surface-volume ratio are reflected by changes in nasal aperture, upper nasal cavity, choana, and nasopharynx breadth and height. Changes in cavity length are described using the relative length of the bony cavity versus that of the nasopharynx. Turbulence enhancing features are reflected in measures of breadth and diameter size step (see Fig. 3).

An extra set of standard landmarks was registered for each specimen to represent overall cranial size (nasal cavity landmarks excluded). These additional landmarks include nasion, glabella, bregma, lambda, inion, basion, radiculare, frontomalare orbitale, zygoorbitale, zygomaxillare, and prosthion. Descriptions of all landmarks follow Bräuer (1988). Each specimen was mounted with plasticine in such

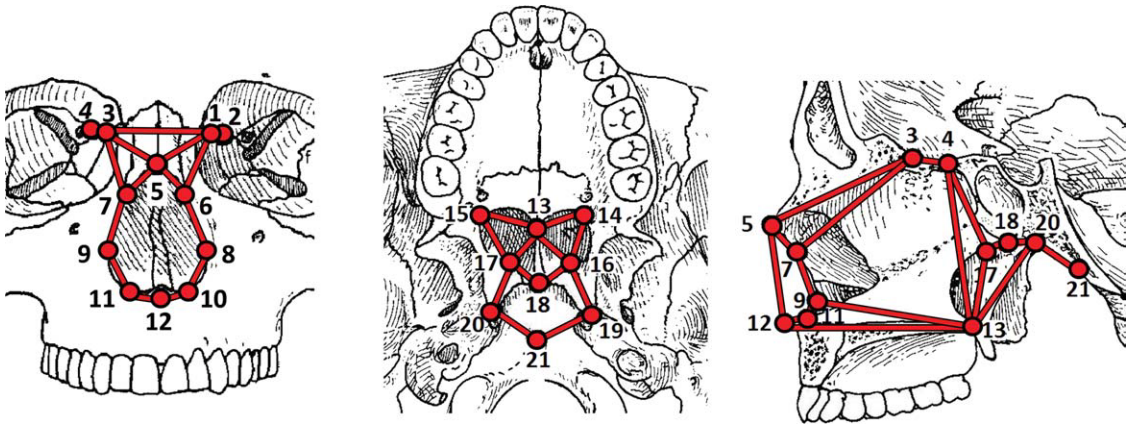

Fig. 2. Locations of the landmarks on schematic representation of lateral (midsagittal cross-section), frontal and inferior views of a human cranium [modified from Bräuer (1988, Figs. 40–42)]. Lines do not represent data; rather they are used to show how landmarks are connected to form a wire frame model, thus enhancing visualization. Numbers correspond to landmark numbers in Table 3. Lines and points are shown in red in the online version. [A color figure can be viewed in the online issue, which is available at wileyonlinelibrary.com].

a way that all landmarks could be obtained in a single series. The specimens preserve all landmarks, except that hormion of three crania had to be estimated because of a damaged vomer.

Error tests

To investigate the intra- and interobserver error, three modern human crania (not part of the comparative samples used) were digitized three times by MN and FS, separately and at different occasions (MN with intervals of 4 and 9 weeks, FS with intervals of 1 day). Following Lockwood et al. (2002), the impact of measurement error on the results was assessed by comparing the Euclidean distances between the repeats of the same individuals to those between all 100 individuals used in the study. These were calculated from the Procrustes coordinate data on all 21 nasal cavity landmarks used in the analyses. Results of the intraobserver error test are shown in Figure 4a. For both authors, the Euclidean distances between repeats (intra FS or intra MN) do not overlap the Euclidean distances between any two different individuals from the actual data set (Total data). This means that intraobserver variation in landmark placement is small relative to inter-individual differences encountered in the full sample analyzed here. The MN measurements show larger Euclidean distances between repeats than those of FS, which may be the result of the longer interval between repeats and less initial familiarity with the measuring procedure.

The effect of interobserver error was assessed by comparing Euclidean distances obtained between repeated measurements taken from the same individuals by both observers to those obtained between the 100 different individual crania used in this research, of which 74 are measured by MN and 26 by FS. The results show minimal overlap in the Euclidean distances (Fig. 4b), with just 54 of 4949 (1%) pairs in the full sample having the same distance range as 6 of 27 (22%) pairs in the interobserver repeat. So 1.09% of the differences in shape measured between two individual crania are similar to differences due to interobserver measurement differences.

The largest Euclidean distances among the interobserver pairs concern initial measurements made by

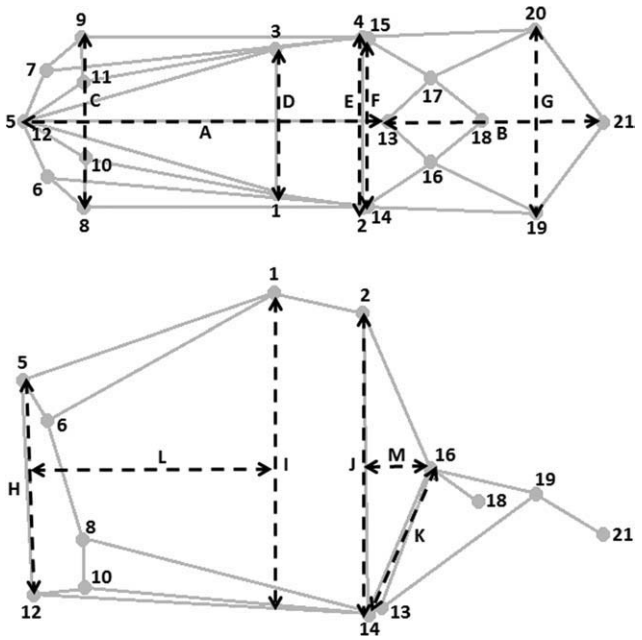

Fig. 3. Locations of the landmarks in the nasal cavity model in superior and lateral view. Numbers correspond to numbers in Fig. 2 and Table 3. Lines indicate measurements used to describe air-wall contact enhancing features and are indicated by letter A–L: (A) Bony cavity length, (B) Nasopharynx length, (C) Nasal aperture breadth, (D and E) Upper nasal cavity breadth, (F) Choana breadth, (G) Nasopharynx breadth, (H) Nasal aperture height, (I and J) Turbinate chamber height, (K) Choana height. The diameter size step anterior cavum-turbinate chamber is described by the difference in height between H and I, relative to the distance between those lines (L). The diameter size step posterior cavum-turbinate chamber is described by the difference in height between K and J, relative to the distance between those lines (M).

MN, suggesting that inexperience with the method could be an underlying factor. The one landmark position particularly prone to interobserver error is the superiormost margin of the choana (landmarks 16, 17). It can be difficult to locate anteroposteriorly, when the

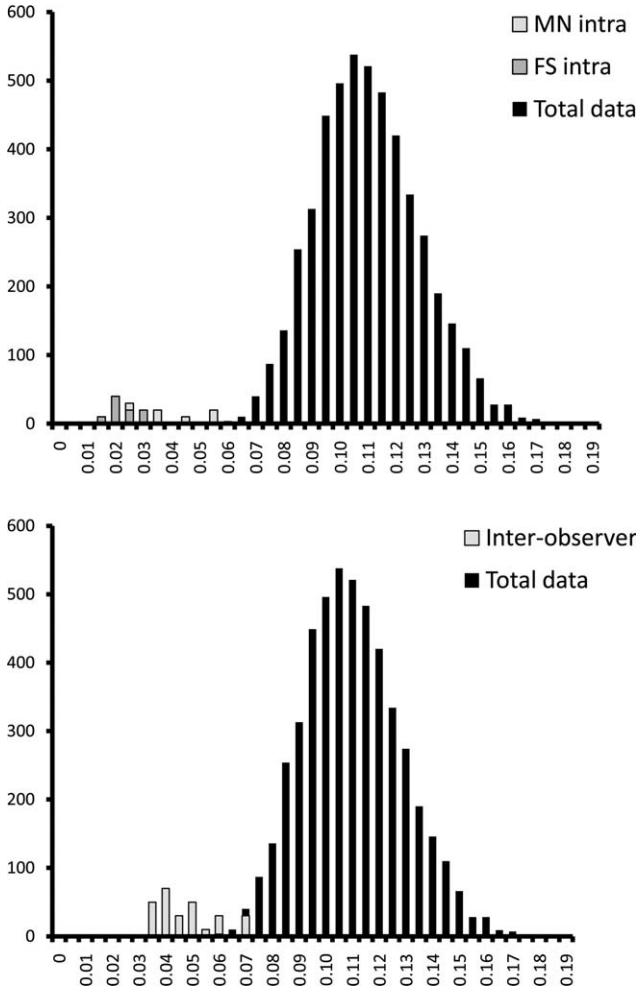

Fig. 4. (**a**) Analysis of intraobserver error. Black columns show frequency distribution of all Euclidean distances among 100 human nasal cavity shapes (total data). Light grey and dark grey columns show the distributions for Euclidean distances between repeats of measurements of MN and FS, respectively. The latter are not to scale and are exaggerated 10 times to illustrate their position relative to differences between individuals (following Lockwood et al., 2002). (**b**) Analysis of interobserver error. Black columns show frequency distribution of all Euclidean distances among 100 human nasal cavity shapes (total data).White columns show the distributions for Euclidean distances between repeats of measurements of the same three crania between both authors. The latter are not to scale and are exaggerated 10 times to illustrate their position relative to differences between individuals.

saddle-shaped area is flat in this direction, and tended to be placed more posteriorly by FS than by MN. The inferosuperior location of landmarks 16 and 17, marking the height of the choanae, is not affected, and these landmarks were kept in the analyses to maintain a biologically meaningful model of the nasal cavity. In the Results section, we will consider if a specific trend in interobserver error could have influenced the results of the analyses.

Statistics

Data superimposition. The three-dimensional coordinates of the 21 nasal landmarks were superimposed with generalized Procrustes analysis (GPA) (Rohlf, 1990; Rohlf and Marcus, 1993; Slice, 1996; O'Higgins and Jones, 1998) using the Morpheus and MorphoJ software packages (Slice, 1998; Klingenberg, 2011). This procedure allowed the visual and statistical assessment of shape after scaling to common centroid size. The fitted coordinates were then used for all further statistical analysis. Centroid size of the nasal cavity (CSnose) was also retrieved from the Procrustes analysis of the nasal cavity landmark set. A similar procedure for the cranial landmark dataset was used to produce a more general, overall cranial measure of size, the centroid size of the cranium (CScran).

Distance matrices. We calculated morphological, climate, and centroid size distance matrices among all 10 groups. We first performed a principal component analysis (PCA) on the Procrustes superimposed coordinates. By using a screeplot, the first eight principal components, accounting for 65.2% of the total variance, were selected to eliminate irrelevant small-scale variation from further analysis (Harvati and Weaver, 2006b). These principal components were then used as variables to calculate Mahalanobis squared distances among our population samples. Mahalanobis D^2 are scaled by the inverse of the pooled covariance matrix and are a measure of the distance between group centroids. (Harvati, 2003; Harvati and Weaver, 2006b; Hubbe et al., 2009). Unlike Procrustes distance, an alternative morphological distance measure used with landmark data, Mahalanobis D^2 accounts for nonindependence of landmark coordinates as well as within-group variation (Neff and Marcus 1980; Klingenberg and Monteiro, 2005). Both PCA and Mahalanobis analyses were performed in SAS (The SAS Institute).

A matrix of squared distances in centroid size was made for both CSnose and CScran. Climate matrices were calculated from the squared differences among series for each climate variable (Tmean, Tmin, Tmax, VPmean, VPmin, VPmax). A geographic distance matrix was also calculated for our population samples, to account for population history, which has been shown to correlate well with geography (see Relethford, 2001). The latter matrix was constructed following Hubbe et al. (2009): geographic distances consisted of linear distances among groups in kilometers, using several checkpoints (Cairo, Bangkok, Bering, and Panama) to confine the distances to terrestrial routes.

Matrix comparisons. To test for patterns of correlation among nasal cavity shape and factors of climate and size we compared the morphological and climatic distance matrices using Mantel Matrix Correlation tests (Mantel 1967; see also Relethford 2004, Harvati and Weaver, 2006a, b; Hubbe et al., 2009) in NTSYSPc, (v2.10t. Applied Biostatistics, Rohlf, 1986–2000). This test evaluates the level of association between two matrices. Permutation tests (10,000 runs) were used to evaluate the significance of the results (Harvati and Weaver, 2006b; Hubbe et al., 2009). Mantel tests also allow for three-way matrix comparisons in a manner similar to a partial correlation among three variables. This enabled us to compare morphological and climate matrices while controlling for the effects of size as well as of geographic distance, used here as a proxy for population history (see also Roseman, 2004; Harvati and Weaver, 2006b; Hubbe et al., 2009).

Partial least squares analysis. To analyze the covariance patterns between nasal cavity shape and climate,

TABLE 4. Mantel correlations results between morphological, climate, and centroid size distances, corrected for geographical distances. Significant correlations ($P < 0.05$) are indicated by *

Nasal cavity shape (first 8PCs) ×		
Temperature	R	p
Mean monthly temperature (Tmean)	0.352	0.026 *
Temperature warmest month (Tmax)	0.287	0.048 *
Temperature coldest month (Tmin)	0.316	0.038 *
Vapor pressure	R	p
Mean monthly vapor pressure (VPmean)	0.308	0.040 *
Vapor pressure wettest month (VPmax)	0.267	0.061 ns
Vapor pressure driest month (VPmin)	0.298	0.048 *
Centroid size	R	p
Nose centroid size (CSnose)	0.388	0.013 *
Cranial centroid size (CScran)	0.236	0.075 ns
Nose centroid size ×		
Temperature	R	p
Mean monthly temperature (Tmean)	0.027	0.397 ns
Temperature warmest month (Tmax)	0.025	0.601 ns
Temperature coldest month (Tmin)	0.018	0.578 ns
Vapor pressure	R	p
Mean monthly vapor pressure (VPmean)	−0.118	0.746 ns
Vapor pressure wettest month (VPmax)	−0.104	0.276 ns
Vapor pressure driest month (VPmin)	−0.124	0.249 ns
Centroid size	R	p
Cranial centroid size (CScran)	0.293	0.040 *
Cranial centroid size ×		
Temperature	R	p
Mean monthly temperature (Tmean)	0.427	0.017 *
Temperature warmest month (Tmax)	0.659	0.997 ns
Temperature coldest month (Tmin)	0.271	0.943 ns
Vapor pressure	R	p
Mean monthly vapor pressure (VPmean)	−0.043	0.592 ns
Vapor pressure wettest month (VPmax)	0.051	0.704 ns
Vapor pressure driest month (VPmin)	−0.094	0.238 ns

we performed a two block partial least squares analysis (2B-PLS) (Bookstein et al., 1990, 2003; Rohlf and Corti, 2000) within MorphoJ. This analysis is particularly useful for analyzing data where there is an expected high degree of multicolinearity within each block (Gil and Romera, 1998). With this analysis, there is no need for an arbitrary choice of factors (Manfreda et al., 2006). This makes PLS analysis ideal for research in a climatic context as temperature and humidity factors in nature are inseparable. The variables in the first block consisted of all six Z-scored climate factors, all of which are highly correlated with each other. Individuals from the same population all had the same value for the climate variables. The second block of variables was formed by first running a second, separate, Procrustes analysis on the raw coordinate data using MorphoJ (Klingenberg, 2011). From the output dataset, only the symmetric component of shape variation was used for further analysis. Asymmetric shape variation, which can also be partly caused by measurement errors, is not of interest for this analysis (Mitteroecker and Gunz, 2009). The 2B-PLS searches for pairs of new explanatory factors (PLS dimensions), one for climate [climate latent variable (LV)], and one for shape (singular warp), that maximize the covariance between the two blocks of data. The first pair of explanatory factors forms the first PLS dimension (PLS1) and explains the highest percentage of the total covariance between the two blocks. Each following PLS dimension consequently explains a lower percentage. The explanatory factors of each dimension are only correlated with each other and not with any factor from other PLS dimensions. The climate LVs scores and singular warp scores can be plotted against each other. This visualizes changes in shape score per change in climate LV score. Each climate LV consists of a combination of the six climate variables. The loadings of the climate variables on the vector of the climate LV show which climate variables are most important for describing the covariation between climate and shape. The loadings of the shape variables on the singular warp can be visualized. This then enables us to describe the shape changes which maximally explain covariance between nasal cavity shape and the optimal combination of climate variables, the climate LV (see also Manfreda et al., 2006). The significance level for the covariation between the blocks and for the correlation between the climate LV and singular warp within each pair of exploratory variables was evaluated using permutation tests (10,000 runs). As the interobserver error was highest for landmarks number 16 and 17 (superiormost margin of choana), we checked the influence of these two landmarks by leaving them out in an extra run of the PLS analysis (described in Results section).

Multiple multivariate regression. To see what shape changes are specifically related to the temperature and vapor pressure factors which had the highest correlation with nasal cavity shape in the Mantel tests and to test whether shape changes related to climate are not only an effect of allometry, we performed a multiple multivariate regression analysis within MorphoJ. The program allows for input of multiple independents (the climate factors and nasal cavity centroid size) and multiple dependents from one dataset (the symmetric component of the Procrustes shape coordinates). Within the program, we can then visualize shape changes related solely to the temperature factor, while the vapor pressure and centroid size are kept constant. We can do the same for shape changes related to vapor pressure. Keeping centroid size constant removes the allometric effect and keeping the other climate factor constant allows for untangling of the separate effects of temperature and humidity.

RESULTS

Correlations

The results of the Mantel tests for correlation between morphological shape distances and climate distances corrected for geographic distance are shown in Table 4. All climate factors, except VPmax, show a significant ($P < 0.05$) correlation with nasal cavity shape. Of the three temperature factors, Tmean has the highest correlation with nasal cavity shape coordinates. Of the three vapor pressure factors, VPmean has the highest correlation with nasal cavity shape. Nasal cavity shape is significantly correlated with nose centroid size. Although there is a significant correlation between nose centroid size (CSnose) and cranial centroid size (CScran), there is no significant correlation between nasal cavity shape and CScran. Centroid size of the nose does not show correlation with either temperature or vapor pressure. Cranial centroid size only shows a highly significant correlation with Tmean.

PLS

To further explore the association between the climate factors and nasal cavity shape, we performed a PLS analysis of the symmetric component of the Procrustes shape coordinates against the Z-scored climate variables (Tmin, Tmax, Tmean, VPmin, VPmax, VPmean). The singular values are 0.043, 0.010, 0.003, 0.0009, 0.0003, and 0.000. The first dimension of the PLS analysis (PLS1) explains 94.3% of the total squared covariance between the shape coordinates and the climate variables. The first two dimensions (PLS1 and PLS2) together span 99.4% of the total squared covariance pattern. The correlation between the first pair of PLS scores (shape vs. climate) is 0.770 ($P = 0.0427$), between the second pair is 0.552 ($P = 0.0217$). The customary permutation test yields a significance level for the first two singular warps of $P < 0.001$ on 10,000 permutations.

Table 5 gives the loadings of the climate LVs on the first two singular vectors: PLS1 and PLS2. It shows that PLS1 is loaded by a combination of positive temperature and positive vapor pressure factors: low PLS1 values indicate cold–dry climate, high PLS1 values indicate warm and humid climate. The highest loading is from Tmean (0.433), but all climate factors have loadings in a similar range (0.392–0.433). PLS2 shows a combination of negatively loading temperature factors and positive loading vapor pressure factors. This means that a high PLS2 score indicates a cold-humid climate, whereas a low PLS2 score indicates a warm and dry climate. PLS2 is mostly loaded by vapor pressure factors, mostly minimum vapor pressure (0.437), but again all climate factors have loadings in a similar range (see Table 5).

On singular warp 1, a clear division is visible between hot–humid climate populations from Gabon and Papua New Guinea which show the highest PLS1 scores, hot–dry climate populations from Australia and South Africa with slightly lower PLS1 scores, and cold climate groups from Tierra del Fuego, the Aleutian Islands, Siberia and Greenland with low PLS1 scores (see Fig. 5). Temperate climate populations from Central Europe and the Chatham Islands show intermediate scores. On singular warp 2, the division is less clear, as all populations overlap. From this graph, it becomes clear that the climatic pattern of PLS1 reflects the hypothesized cline in climatic stress.

Shape changes. Because PLS1 already explains 94.3% of the covariance between nasal cavity shape and the climatic factors, description of shape changes will only focus on the first singular warp. Figure 6 shows the first singular warp against the first climate LV score. Although there is intrapopulation variation, there is a significant correlation [$r = 0.77$, P (perm.) = 0.0427] between the first pair of PLS scores, with higher than average nasal shape scores in populations with high climate LV scores (e.g., Gabon, Papua New Guinea, Australia) and low nasal shape scores in populations with low climate LV scores (e.g., Siberia, Greenland).

Shape changes related to PLS1 are summarized in Figure 7. There are three regions of the nasal cavity that show shape variation: 1) Nasal aperture, 2) Upper nasal cavity, and 3) Nasopharynx. Compared with high scoring populations (e.g. warm and humid climates), populations with low PLS1 scores (colder and drier climates) show a superior shift of rhinion, an inferior shift of the anterior nasal spine and a closer to midline positioning of the nasale landmarks and most inferior margins of the nasal aperture. This results in a relatively higher and narrower nasal aperture (see Fig. 7). Furthermore, cold–dry climate populations have anterior and posterior ethmoid foramina positioned more superiorly and closer to midline. The anterior foramina are more closely spaced than the posterior ones. This gives the appearance of a relatively high and narrow upper nasal cavity. In total, the landmarks of the nasal cavity landmarks show a high and anteriorly narrowing nasal cavity shape. The superiormost margins of the choanae are located more posteriorly which increases the relative posterior cavum length. The more anteriorly positioned pharyngeal tubercle and more posterior positioned posterosuperior ends of the medial pterygoid plates shorten the nasopharynx. Width of the nasopharynx does not show variation, neither does height.

TABLE 5. Loadings of the first two PLS vectors for the climate latent variables

	PLS1	PLS2
Tmean	0.433	−0.394
Tmin	0.417	−0.349
Tmax	0.430	−0.422
VPmean	0.392	0.434
VPmin	0.376	0.437
VPmax	0.400	0.407

Multiple multivariate regression

To examine the separate effects of temperature and vapor pressure on nasal cavity shape, corrected for effects of allometry, the nasal cavity shape coordinates are regressed on Z-scored Tmean, Z-scored VPmean and CSnose simultaneously. Only a small percentage of the total variance within the sample can be explained by Tmean (6.65%) and VPmean (5.48%). Centroid size, however, explains an even smaller amount (3.52%). Together the three factors explain 13.17%, indicating that there is some overlap in the morphology that the factors explain. Pearson correlation between regression scores and VPmean (with Tmean and Cnose kept constant) is lower ($r = 0.23$, $p = 0.025$) than the correlation between regression scores and Tmean (with VPmean and Cnose kept constant) ($r = 0.44$, $P < 0.001$). This could indicate that vapor pressure has only a minor contribution to shape variation and that most of its correlation with shape is due to its high colinearity with temperature.

Shape changes Tmean. Visualizations of the nasal cavity shape changes related to Tmean, corrected for VPmean and CSnose effects, are shown in Figure 8. Compared with warm climates, nasal cavities from cold climates show a superior shift of rhinion and the nasomaxillare landmarks, an inferior-posterior shift of the anterior nasal spine, left and right alare, and the inferiormost margins of the nasal aperture. The last two sets of landmarks are also located closer to the midline. This results in a higher and much narrower nasal aperture. Furthermore, cold climate nasal cavities show a superior-anterior and closer to the midline position of the anterior ethmoid foramen, as well as a closer to the midline position of the posterior ethmoid foramen. These landmark shifts indicate an anteriorly narrower and longer upper nasal cavity. Overall, the nasal cavity of cold populations is laterally narrowing from back to the front, compared with a widening in warm climate nasal cav-

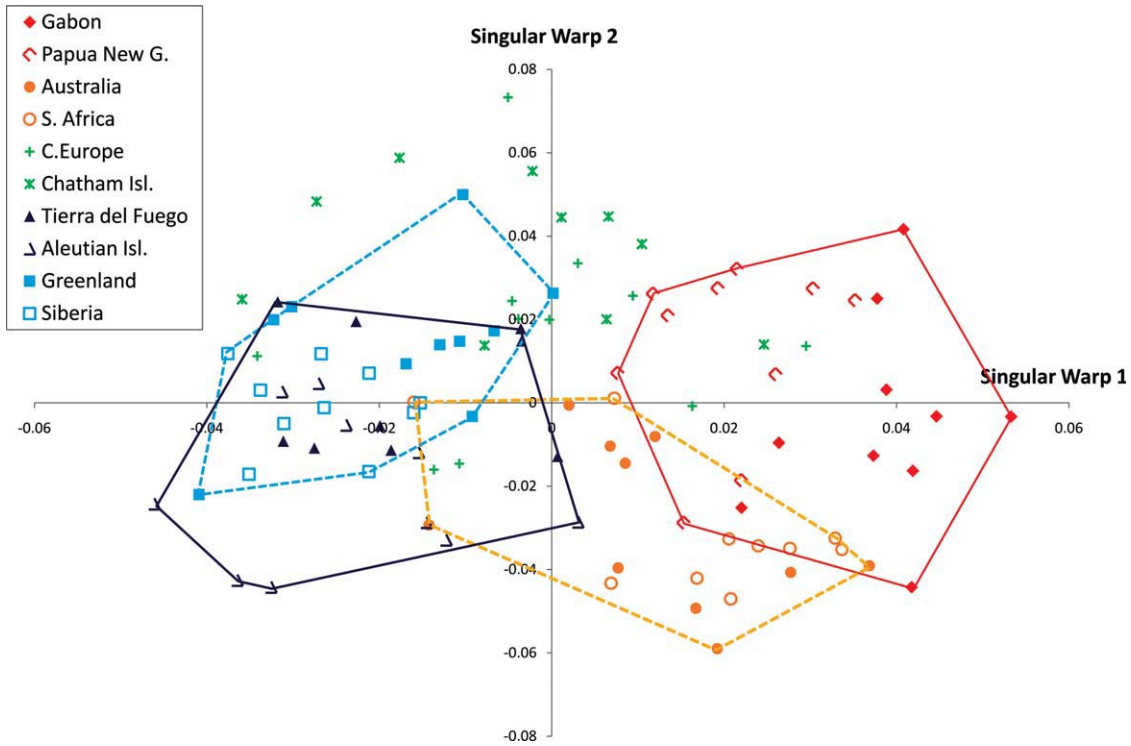

Fig. 5. First two singular warp scores for the shape coordinates, with convex hulls marking the cold–dry (turquoise dashed line), cold–humid (dark blue line), hot–dry (orange dashed line) and hot–humid (red line) populations. Note that grouping of the populations on singular warp 1 corresponds with the climate latent variable 1 scores: cold populations have low PLS1 scores (left two convex hulls), warm populations have high PLS1 scores (right two convex hulls).

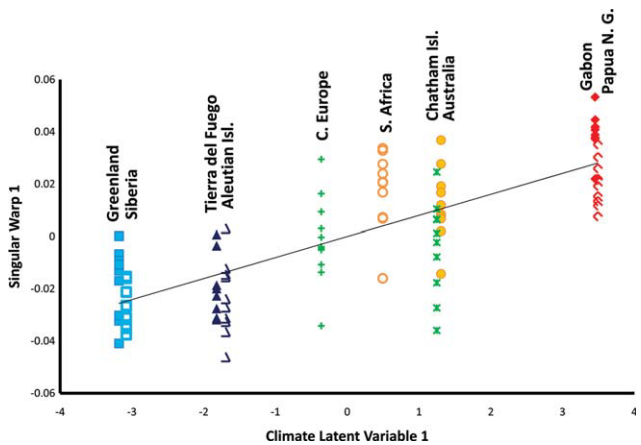

Fig. 6. PLS1: shape scores (singular warp 1) versus climate latent variable scores (climate LV1). Color legend: see Figure 5.

ities (Fig. 8, superior view). At the nasopharynx, several landmarks change: an inferior shift of the inferolateral choanal corners combined with a superior shift of the superiormost margins of the choanae increases choanae height, an anterior shift of hormion, an inferior shift of the posterosuperior end of the medial pterygoid plates and a posterior-inferior shift of the pharyngeal tubercle. This indicates a relatively elongated nasopharynx shape with a smoother, less abrupt diameter size step from nasopharynx to the posterior cavum due to high choanae.

Shape changes VPmean. Visualization of the shape changes related to VPmean (see Fig. 9), corrected for Tmean and CSnose effects, shows nasal cavity shape differences between dry and humid climates. Compared with humid climates, dry climate nasal cavities show an inferior shift of rhinion and nasomaxillare, a superior shift of the anterior nasal spine and inferiormost margins of the nasal aperture, a posterior-inferior shift of the anterior ethmoid foramen and superiormost margins of the choanae, a superior shift of the posterior ethmoid foramen and an superior-anterior shift of the pharyngeal tubercle. Overall, these shifts result in lower nasal apertures in dry climates, with the nasal cavity tapering more strongly from posterior to anterior compared with nasal cavities in humid climates. The nasopharynx in dry climates is shortened, while the posterior cavum is elongated. The diameter size step from nasopharynx to posterior cavum is more abrupt in dry climate, due to higher posterior cavum, lower choanae, and shorter nasopharynx.

Shape changes CSnose. The shape changes related to differences in nasal cavity size (CSnose with Tmean and VPmean kept constant) are shown in Figure 10. Overall, shape differences between the smallest and largest nasal cavities in the measured sample are relatively small compared with the climate-related changes. No changes in width of the cavity are observed. Compared with small nasal cavities, large noses show an anterior-superior shift of rhinion, an anterior-inferior shift of the anterior nasal spine, a posterior shift of nasale, and an anterior-inferior shift of the pharyngeal tubercle.

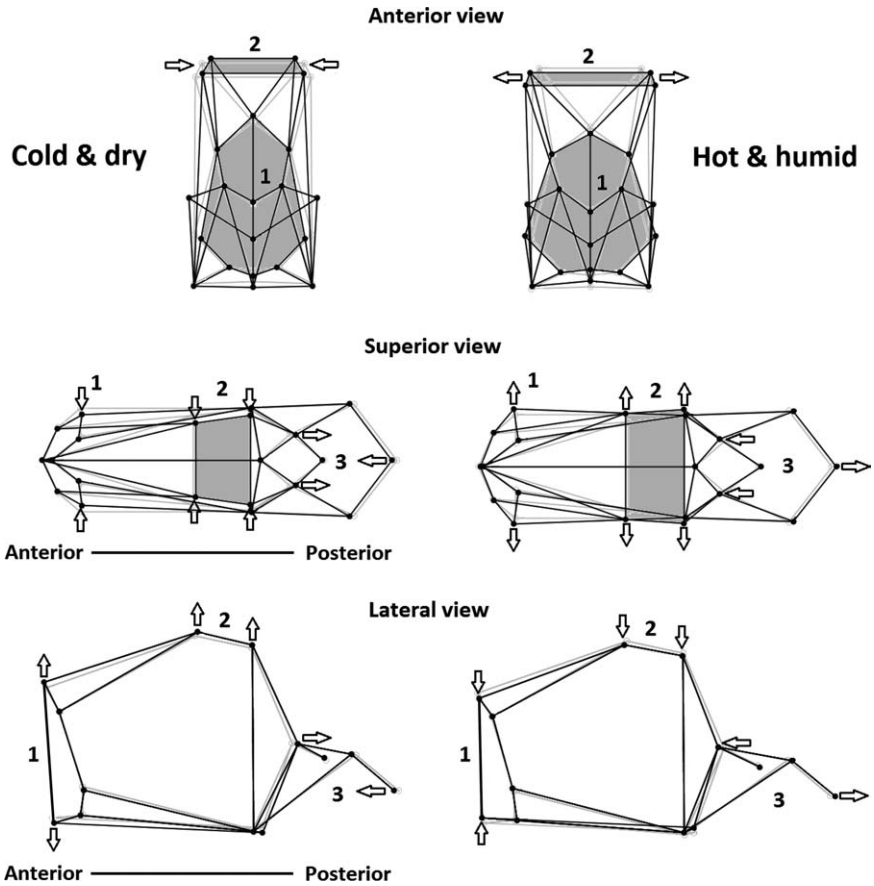

Fig. 7. Comparing shape differences between low scoring populations "cold and dry" (−0.04 on singular warp 1) and high scoring populations "warm and humid" (0.04 on singular warp 1). Showing anterior, superior, and lateral view of the nasal cavity wireframe model. Light grey colored frame indicates average cavity shape. Areas with most shape change are indicated by arrows and/or colored grey for visualization purposes. Numbers correspond with the described three regions of morphological change: 1. Nasal aperture, 2. Upper nasal cavity, and 3. Nasopharynx.

In all, the shape changes related to a trend from cold–dry to hot–humid climates shown by the PLS analysis (see Fig. 7) appear to combine two separate shape trends visible in the Multiple regressions on Tmean and VPmean (Figs. 8 and 9). The bony cavity itself is mostly associated with temperature, whereas the nasopharynx is mostly associated with humidity. In addition, there is a small allometric effect shown in both analyses.

Effects of interobserver error

Comparing the results obtained here with the findings of the error test suggests that the outcome of the analyses is not biased by interobserver error. There is no clear difference in PLS1 singular warp scores between the two cold–dry populations (see Fig. 6), even though one was measured by FS (Siberia), and the other near-exclusively by MN (Greenland). The same can be seen for the two cold-humid populations, with one measured by FS (Aleutian Islands), and the other near-exclusively by MN (Tierra del Fuego).

Second, we examined the impact of the one landmark position most prone to interobserver error, the superior-most choanal margin (landmark 16, 17). Re-running the PLS analysis leaving out these landmarks, does not change the results in any substantial way. PLS1 still captures the morphological differences between cold–dry versus hot–humid climate groups, and all shifts in landmarks are the same (not shown here). The RV coefficient becomes slightly lower (0.208 instead of 0.225) and the first PLS explains 94.6% of the total covariation within the sample (instead of 94.3%). The correlation between the two blocks becomes slightly smaller (0.74 instead of 0.77).

Third, FS measured 59% of the cold sample, but only 8% of hot sample. In the error test, he tended to place landmarks 16 and 17 more posteriorly than MN. Hence, if cold populations would show a trend toward a more posterior position of these landmarks this could indicate a bias caused by interobserver error. However, the multiple regression analyses show that the anteroposterior position of landmarks 16 and 17 is not correlated with Tmean (see Fig. 8). It is correlated with VPmean (see Fig. 9), but FS measured near-equal parts of the humid and dry samples.

DISCUSSION

Hypothesis 1: correlations of climate with cavity shape

Our first hypothesis is that there is a relationship between climate and nasal cavity shape. The predictions of this hypothesis were met by our results. We found significant correlations between nasal cavity shape and

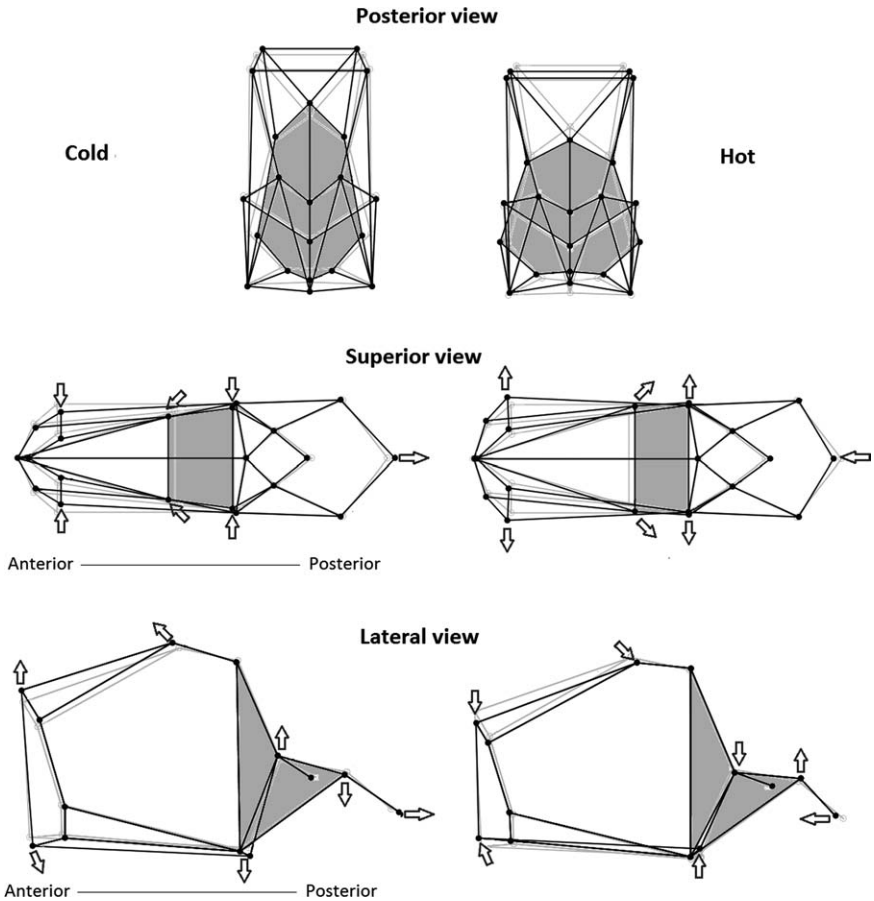

Fig. 8. Comparing nasal cavity shape differences along regression on Tmean: cold climate morphology (left) versus hot climate morphology (right). Showing posterior, inferior, and lateral views of the nasal cavity wireframe model. Light grey colored frame indicates average cavity shape. Areas with most shape change are marked in grey for visualization purposes.

climatic factors of temperature and vapor pressure. This supplements earlier research that found significant correlations between temperature and the human face (Harvati and Weaver, 2006b; Hubbe et al., 2009). Harvati and Weaver (2006b) found no significant correlations between vapor pressure and shape of the face. However, that study used no nasal landmarks. Hubbe et al. (2009) reported significant correlations between nasal measurements (breadth and height of the nasal aperture) and all the temperature variables used, as well as two of the humidity measures (annual rainfall and rainfall of the wettest month; vapor pressure was not used in that study). Our findings indicate that the nasal capsule might be more strongly responding to climate, especially vapor pressure, compared with the rest of the face. This supports the notion that the nasal capsule forms a functional unit with a degree of independence from the rest of the face (Carey and Steegmann, 1981). From both temperature and vapor pressure factors, the mean monthly values were most highly correlated with nasal cavity shape. The PLS analysis showed that all climate factors have a similar loading on the first PLS. This suggests that the minimum and maximum values of the climate variables follow similar patterns as the mean values. Yearly variability, e.g., the amount of difference between minimum and maximum temperatures thus does not seem to play an important role in nasal cavity shape.

The second prediction, that trends in nasal cavity shape follow climatic trends of increased difficulty of air-conditioning: from hot–humid to cold–dry, was also supported. From the PLS analysis it is shown that nasal cavity shape depends on a combination of both temperature and vapor pressure factors. Maximum covariation between nasal cavity shape and climatic factors follows a cline from hot–humid to cold–dry climate, via hot–dry and cold–humid climate. Temperate populations score intermediate. Although vapor pressure and temperature factors both have similar loadings on the first PLS dimension, the grouping of the populations indicates that the main difference in shape is related to temperature (see Fig. 5). This contradicts the notion that humidity should play a more important role in nasal climate adaptation, as humidification is a more important factor for air-conditioning than temperature adjustment (Negus, 1958).

Considering our hypothesis that dry and cold climate would be the most difficult to condition air, we assumed that nasal cavity shape would follow similar adaptive trends toward more dry and towards more cold climates when humidity and temperature are considered separately. This, however, appears not to be the case. The multiple regression analysis showed that

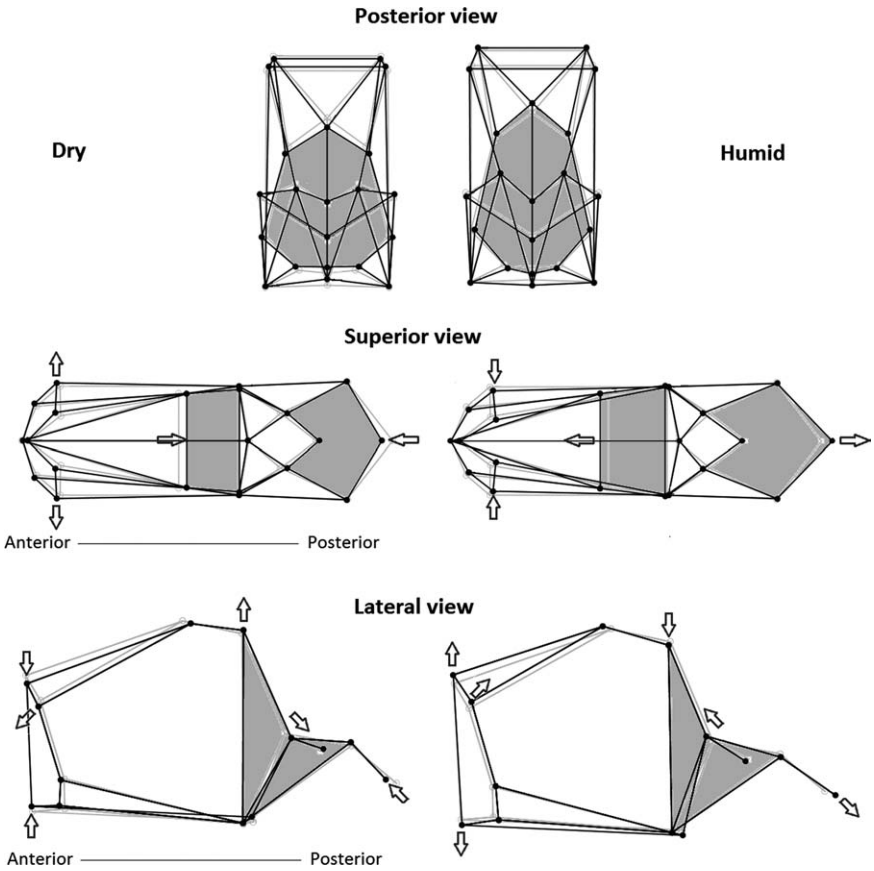

Fig. 9. Comparing nasal cavity shape differences along regression on VPmean: dry climate morphology (left) versus humid climate morphology (right). Showing posterior, inferior, and sagittal views of the nasal cavity wireframe model. Light grey colored frame indicates average cavity shape. Areas with most shape change are marked in grey for visualization purposes.

vapor pressure and temperature have opposite effects on nasal cavity shape (Figs. 8 and 9). For example, cold climates are related to higher nasal cavities with high nasal apertures and choanae, and elongated upper nasal cavities, whereas dry climates are related to lower nasal cavities with low nasal apertures and shortened upper nasal cavities. The nasal cavity shape effect of temperature seems to be focused on increasing turbulence during inspiration by the anterior narrowing of the nasal cavity and increased air-wall contact by a relatively longer upper nasal cavity in colder climates. The vapor pressure effect seems twofold: an increase in the turbinate chamber length relative to the nasopharynx and a focus on moisture retention during expiration in drier climates, with a larger diameter size step from nasopharynx to turbinate chamber. When combining both separate shape trends one can arrive at a morphology as shown by the PLS analysis. Although the multiple multivariate regression analysis can be used to study the separate effects of temperature and humidity on nasal cavity shape, our results suggest that there might be a problem with analyzing influence of factors with such high colinearity. It can be questioned how useful this untangling of climate factors is, as in nature temperature and vapor pressure are inseparable. A functional interpretation of the shape changes will therefore only be discussed for the PLS results.

Combining the temperature and vapor pressure effects in the PLS analysis (see Fig. 7), and comparing this with the separate shape changes in the regression analysis (Figs. 8 and 9), it appears that in cold–dry climates it is cold temperatures that most influence the nasal aperture and anterior narrowing of the cavity, whereas it is the low vapor pressure that has a stronger influence on the nasopharynx. Both climatic factors cause a superior shift of the ethmoid foramen, which makes an extra high upper nasal cavity in cold–dry climates. It seems that a higher turbinate area might indeed be very important for air-conditioning (Uliyanov, 1998; Franciscus, 2003).

Finally, we predicted that the relationship between climate and nasal cavity shape would hold irrespective of size differences. After correction for allometry nasal cavity shape is still correlated with temperature and vapor pressure, as predicted (Figs. 8 and 9). Although nasal cavity shape is significantly correlated with nose centroid size (Table 4), nose centroid size is neither correlated with temperature nor with humidity (Table 4: Tmean, VPmean). Therefore, it is unlikely that these climatic factors primarily affect nasal cavity size and shape via allometric effects. Multiple multivariate regression analysis shows that there are only minor shape changes that are related to nose centroid size (after correction for Tmean and VPmean; see Fig. 10). Those shape changes are only related to the height of the nasal aperture (not the width), and the position of the pharyngeal tubercle.

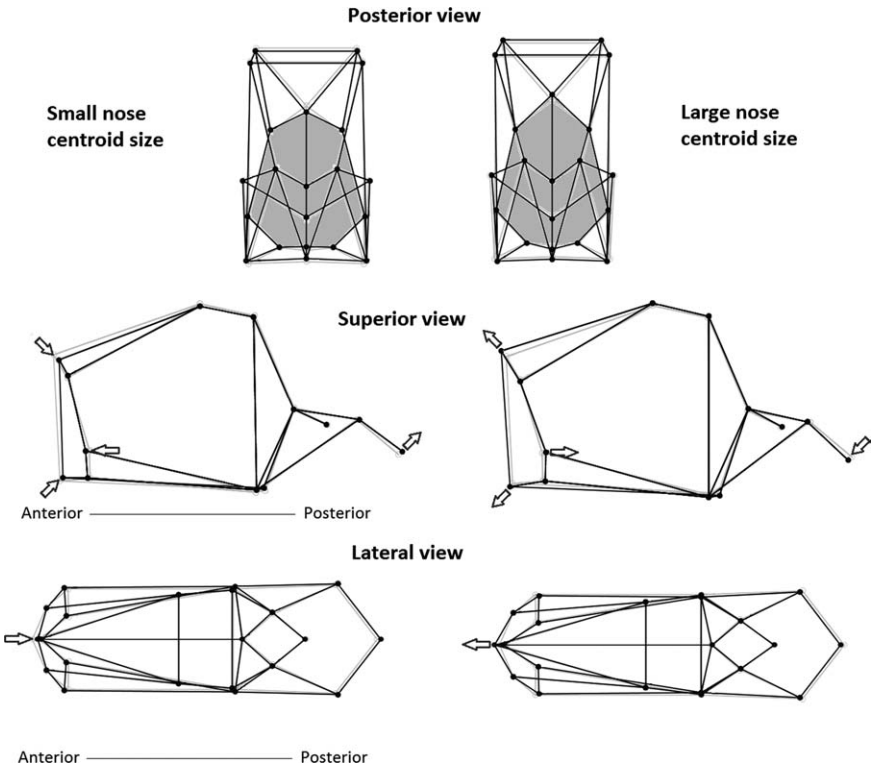

Fig. 10. Comparing nasal cavity shape differences along regression on Cnose (Tmean and VPmean kept constant): small nose morphology (left) versus large nose morphology (right). Showing posterior, inferior, and sagittal views of the nasal cavity wireframe model. Light grey colored frame indicates average cavity shape. Arrows indicate areas of largest shape changes.

They do not affect the width of the cavity, nor the height. After correction for centroid size, the shape changes remain visible for Tmean and VPmean. This indicates that the climatic effects observed in the PLS analysis are indeed not the result of allometry. As nasal cavity size, Tmean and VPmean together only explained 13.17% of the total nasal cavity shape variation, about 67% of the total variation remains unexplained within current research. This might indicate importance of other factors such as turbinate morphology, soft tissue differences, influence of diet, lifestyle, age, and/or sex.

Hypothesis 2: cold–dry climate groups and air-wall contact

In nature, vapor and temperature effects are not separable. Therefore, a functional interpretation of nasal cavity morphology can only be given for the PLS results (and not for the regression results), as these provide a realistic overview of the combined effects of temperature and vapor pressure. Table 6 summarizes the changes in hypothesized turbulence and contact time enhancing features in nasal cavity shape in hot–humid and cold–dry climate.

We predicted an increase in air-wall contact enhancing features in cold–dry climate populations (turbulence, contact time, surface-volume ratio). Concerning this prediction, nasal cavity morphology does show an increase in air-wall contact with increasing difficulty of air-conditioning in physiologically more demanding environments (Fig. 7, Table 6).

Cold–dry climate populations show a decrease in upper nasal cavity width, which increases surface/volume ratio in this part of the cavity. This confirms previous findings of a narrower superior ethmoidal breadth in supra-Saharan populations compared with sub-Saharan Bantu groups at any given interorbital width (Franciscus, 2003). The particular importance of the relatively narrower upper parts of the nose in conditioning of the air has previously been pointed out by Uliyanov (1998). The breadth of the upper nasal fossa might well be one of the critical internal nasal features for climate adaptation (Franciscus, 2003). The observed increased height in combination with a narrower upper nasal cavity in cold–dry populations in our study could thus be related to the need to create such a narrow space with a high surface-volume ratio for air-conditioning, while keeping the nasal resistance sufficiently low. Furthermore, a relatively decreased length of the nasopharynx in cold–dry populations might indicate increased importance of the rest of the nasal cavity for air-conditioning functions. The actual area of air-conditioning (nasal valve and turbinate chamber) (Keck et al., 2000) is relatively reduced in the hot–humid climate groups and increases in size in colder and drier climate populations.

Our results also showed an anterior widening of the nasal cavity in hot–humid climate populations. This finding was not among the predictions of our hypotheses. During expiration, this nasal shape might result in reduced air-nose contact, reflecting the reduced need to retain moisture. In cold–dry populations the anterior part of the cavity is relatively narrow. This nasal aperture shape might cause an increased surface/volume ratio in the nasal entrance and could act as a mechanism to increase warmth and moisture conservation (Shea, 1977).

TABLE 6. Overview of contact time enhancing (+) or decreasing (−) features in populations from cold–dry and hot–humid climates

Feature		Cold–dry		Hot–humid
High surface-volume ratio	+	Narrow superior cavity	−	Wide superior cavity
	+	Narrow nasal aperture	−	Wide nasal aperture
Long cavity length	+	Long bony cavity relative to nasopharynx length	−	Short bony cavity relative to nasopharynx length
High turbulence	+	Higher cavity and nasal aperture	−	Lower cavity and nasal aperture
	+	Increased anterior degree of increase in cross-sectional area	−	Decreased anterior degree of increase in cross-sectional area
	+	Anterior narrowing cavity	−	Anterior broadening cavity
	−	Narrow nasal aperture	+	Wide nasal aperture
	−	Decreased degree of increase in posterior cross-sectional area	+	Increased posterior degree of increase in cross-sectional area

Our study further found that cold–dry nasal cavities do indeed show an increase of features that enhance turbulence (see Fig. 7). The expected features in such environments (larger diameter of the cavity, especially cavity height, and a pronounced diameter size step from anterior and posterior cavum to the turbinate chamber) are found within the cold–dry population samples (see Table 6). A higher cavity would result in an increase in turbulence due to its large diameter (Churchill et al., 2004). A large diameter size step has been found to result in greater air turbulence (Mlynski et al. 2001). The inflow tract from the nostrils (not measured here) to the high nasal aperture of cold–dry populations might form an extra diameter size step at the nasal cavity entrance, creating a high level of turbulence immediately after inspiration.

Contrary to our expectations, some turbulence enhancing features are also found in hot–humid climates (see Table 6). Importantly, hot–humid groups have a relatively large diameter size step from the posterior cavum to the turbinate chamber, which increases turbulence in the nasal cavity during expiration (Mlynski et al., 2001). Such morphology could be expected in hot–dry climate groups and in cold groups to increase moisture retention during expiration (Franciscus and Trinkaus, 1988; Clement and Gordts, 2005). Its occurrence here in hot–humid groups seems contradictory. The wide nasal aperture might create more turbulence during inspiration, but its presence might be related to the reduction of contact time between the air and mucosal tissue.

Our results further show that populations from hot–humid climates have a relatively lower overall nasal cavity. The observed decrease in overall height is a turbulence restricting feature, as a low diameter of a tube enhances laminar flow (Churchill et al., 2004). Laminar flow is the most energy efficient way of breathing and is therefore expected to occur in environments where neither warming nor humidification of the air is necessary (Churchill et al., 2004). This shape, however, also increases surface/volume ratio which is an unexpected feature in climates where air-conditioning is relatively easier.

For this article, we focused explicitly on the function of the nasal cavity in conditioning the air to maintain lung function. However, other functions of the nose, such as filtering, olfaction and a possible role in thermoregulation, might also affect nasal cavity shape. If we assume that the nasal cavity plays a role in heat loss, the observed morphology in hot and humid climate might be interpreted as a way of increasing contact with the moist mucosal tissue to promote local evaporative cooling (Mariak et al. 1999). However, besides nasal cavity dimensions, an important factor influencing the available surface would be the structure and size of the turbinates. Future studies including internal measurements might clarify this issue further.

Although this study documents clear trends in nasal cavity shape, there is much intrapopulation variation and overlap among populations, especially in the intermediate climate groups. Furthermore, the observed differences are modest, perhaps because nasal shape is a compromise of its different functions (Churchill et al., 2004), or because extreme adaptations would reduce the versatility of humans as generalists and a mobile species.

CONCLUSIONS

Our study found significant correlations between nasal cavity morphology as reflected by our dataset and both temperature and vapor pressure variables. The bony nasal cavity appears mostly associated with temperature, and the nasopharynx with humidity. Most importantly, nasal cavities from cold–dry climates are relatively higher and narrower compared with those of hot–humid climates, agreeing with previous findings on the nasal aperture. The shape changes found are functionally consistent with an increase in contact between air and mucosal tissue in cold–dry climates by increase of turbulence during inspiration and increase in surface-to-volume ratio in the upper nasal cavity. However, the observed shape differences are relatively modest and show population overlap, which might indicate a compromise morphology of the nasal cavity and/or the absence of extreme adaptations that would reduce the versatility of humans as generalists and a mobile species. Future study including internal measurements and larger/more diverse population samples will further refine our findings and improve our understanding of the role of the nasal cavity in modern human climate adaptation.

ACKNOWLEDGMENTS

We thank Chris Stringer, Rob Kruszynski, Ian Tattersall, and Giselle Garcia for allowing access to the cranial material and for sharing their knowledge on the collections. We are also grateful to Susan Antón, Markus Bastir, Fred Bookstein, Will Harcourt-Smith, Mark Hubbe, Chris Klingenberg, the late Charles Lockwood, Paul O'Higgins, Geert Jan van Oldenborgh, Christophe Soligo, and Martin Todd for helpful discussion and advice. We thank the Editor and Associate Editor of the American Journal of Physical Anthropology and two anony-

mous reviewers. Their comments and suggestions greatly improved this manuscript.

LITERATURE CITED

Baker PT. 1988. Human adaptability. In: Harrison GA, Tanner JM, Pilbeam DR, Baker PT, editors. Human biology: an introduction to human evolution, variation, growth and adaptability. Oxford: Oxford University Press. p 437–547.

Beals KL, Courtland LS, Dodd SM, Angel JL, Armstrong E, Blumenberg B, Girgis FG, Turkel S, Gibson KR, Henneberg M, Menk R, Morimoto I, Sokal RR, Trinkaus E. 1984. Brain size, cranial morphology, climate, and time machines [and comments and reply]. Curr Anthropol 25:301–330.

Bookstein FL. 1991. Morphometric tools for landmark data. New York: Cambridge University Press.

Bookstein FL, Gunz P, Mitteroecker P, Prossinger H, Schaefer K, Seidler H. 2003. Cranial integration in *Homo*: singular warps analysis of the midsagittal plane in ontogeny and evolution. J Hum Evol 44:167–187.

Bookstein, FL, Sampson, PD, Streissguth AP. 1996. Exploiting redundant measurement of dose and developmental outcome: new methods from the behavioral teratology of alcohol. Dev Psychol 32:e404–e415

Bräuer G. 1988. Osteometrie. In: Knußmann R, editor. Anthropologie—Handbuch der vergleichenden Biologie des Menschen. Stuttgart: Gustav Fischer Verlag. p 160–232.

Cabanac M, Caputa M. 1979. Natural selective cooling of the human brain: evidence of its occurrence and magnitude. J Physiol 286:255–264.

Carey JW, Steegmann AT. 1981. Human nasal protrusion, latitude, and climate. Am J Phys Anthropol 56:313–319.

Churchill SE, Shackelford LL, Georgi JN, Black MT. 2004. Morphological variation and airflow dynamics in the human nose. Am J Hum Biol 16:625–638.

Clement PAR, Gordts E. 2005. Consensus report on acoustic rhinometry and rhinomanometry. Rhinology 43:169–179.

Cole P. 1982. Upper respiratory airflow. In: Proctor DF, Andersen IB, editors. The nose: upper airway physiology and the atmospheric environment. Amsterdam: Elsevier Biomedical Press. p 163–189.

Cole P. 2000. Biophysics of nasal airflow: a review. Am J Rhinol 14:245–249.

Corey JP, Gungor A, Nelson R, Liu XL, Fredberg J. 1998. Normative standards for nasal cross-sectional areas by race as measured by acoustic rhinometry. Otolaryngol Head Neck Surg 119:389–393.

Courtiss EH, Goldwyn RM. 1983. The effects of nasal surgery on air-flow. Plast Reconstr Surg 72:9–19.

Davies A. 1932. A re-survey of the morphology of the nose in relation to climate. J R Anthropol Inst 62:337–359.

Dean MC. 1988. Another look at the nose and the functional significance of the face and nasal mucous membrane for cooling the brain in fossil hominids. J Hum Evol 17:715–718.

Deklunder G, Dauzat M, Lecroart JL, Hauser JJ, Houdas Y. 1991. Influence of ventilation of the face on thermoregulation in man during hyperthermia and hypothermia. Eur J Appl Physiol 62:342–348.

Franciscus RG. 2003. Comparing internal nasal fossa dimensions and classical measures of the external nasal skeleton in recent humans: inferences for respiratory airflow dynamics and climatic adaptation. Am J Phys Anthropol Suppl 36:96–97.

Franciscus RG, Long JC. 1991. Variation in human nasal height and breadth. Am J Phys Anthropol 85:419–427.

Franciscus RG, Trinkaus E. 1988. Nasal morphology and the emergence of *Homo erectus*. Am J Phys Anthropol 75:517–527.

Gil JA, Romera R. 1998. On robust partial least squares (PLS) methods. J Chemomet 12:365–378.

Hall RL. 2005. Energetics of nose and mouth breathing, body size, body composition, and nose volume in young adult males and females. Am J Hum Biol 17:321–330.

Harvati K. 2003. The Neanderthal taxonomic position: models of intra- and inter-specific craniofacial variation. J Hum Evol 44:107–132.

Harvati K, Weaver T. 2006a. Reliability of cranial morphology in reconstructing Neanderthal phylogeny. In: Hublin J-J, Harvati K, Harrison T, editors. Neanderthals revisited: new approaches and perspectives. Netherlands: Springer. p 239–254.

Harvati K, Weaver TD. 2006b. Human cranial anatomy and the differential preservation of population history and climate signatures. Anat Rec A 288:1225–1233.

Hubbe M, Hanihara T, Harvati K. 2009. Climate signatures in the morphological differentiation of worldwide modern human populations. Anat Rec A 292:1720–1733.

Inthavong K, Tian ZF, Tu JY. 2007. CFD simulations on the heating capability in a human nasal cavity. In: Jacobs P, McIntyre T, Cleary M, Buttsworth D, Mee R, Clements R, Morgan R, Lemckert C, editors. Proceedings of the 16th Australasian Fluid Mechanical Conference (AFMC). Gold Coast, Queensland, Australia. p 842–847.

Jessen C, Kuhnen G. 1992. No evidence for brain-stem cooling during face fanning in humans. J Appl Physiol 72:664–669.

Keck T, Leiacker R, Heinrich A, Kuhnemann S, Rettinger G. 2000. Humidity and temperature profile in the nasal cavity. Rhinology 38:167–171.

Klingenberg CP. 2011. MorphoJ: an integrated software package for geometric morphometrics. Mol Ecol Res 11:353–357.

Klingenberg CP, Monteiro LR. 2005. Distances and directions in multidimensional shape spaces: implications for morphometric applications. Syst Biol 54:678–688.

Lieberman DE. 2011. The evolution of the human head. Cambridge, MA: Belknap Press.

Lockwood CA, Lynch JM, Kimbel WH. 2002. Quantifying temporal bone morphology of great apes and humans: an approach using geometric morphometrics. J Anat 201:447–464.

Maloney SK, Mitchell D, Mitchell G, Fuller A. 2007. Absence of selective brain cooling in unrestrained baboons exposed to heat. Am J Physiol Regul Integr Comp Physiol 292:R2059–R2067.

Manfreda E, Mitteroecker P, Bookstein FL, Schaefer K. 2006. Functional morphology of the first cervical vertebra in humans and nonhuman primates. Anat Rec B 289:1552–4906.

Mantel N. 1967. Detection of disease clustering and a generalized regression approach. Cancer Res 27:209–220.

Mariak Z, White MD, Lewko J, Lyson T, Piekarski P. 1999. Direct cooling of the human brain by heat loss from the upper respiratory tract. J Appl Physiol 87:1609–1613.

Mekjavic IB, Rogelj K, Radobuljac M, Eiken O. 2002. Inhalation of warm and cold air does not influence brain stem or core temperature in normothermic humans. J Appl Physiol 93:65–69.

Mitteroecker P, Gunz P. 2009. Advances in geometric morphometrics. Evol Biol 36:235–247.

Mlynski G, Grutzenmacher S, Plontke S, Mlynski B, Lang C. 2001. Correlation of nasal morphology and respiratory function. Rhinology 39:197–201.

Morgan NJ, Macgregor FB, Birchall MA, Lund VJ, Sittampalam Y. 1995. Racial differences in nasal fossa dimensions determined by acoustic rhinometry. Rhinology 33:224–228.

Mowbray K, Gannon PJ. 2001. Unique anatomy of the Neanderthal skull. Athena Rev 4:59–64.

Neff NA, Marcus LF. 1980. A survey of multivariate methods for systematics. New York: Privately published.

Negus V. 1958. The comparative anatomy and physiology of the nose and paranasal sinuses. Edinburgh: E. & S. Livingstone Ltd.

O'Higgins P, Jones N. 1998. Facial growth in *Cercocebus torquatus*: an application of three dimensional geometric morphometric techniques to the study of morphological variation. J Anat 193:251–272.

Relethford JH. 2001. Global analysis of regional differences in craniometric diversity and population substructure. Hum Biol 73:629–636.

Relethford JH. 2004. Boas and beyond: migration and craniometric variation. Am J Hum Biol 16:379–386.

Rohlf FJ. 1990. Rotational fit (Procrustes) methods. In: Rohlf FJ, Bookstein FL, editors. Proceedings of the Michigan Morphometrics Workshop. Ann Arbor: University of Michigan Museum of Zoology. p 227–236.

Rohlf FJ, Corti M. 2000. Use of two-block partial least-squares to study covariation in shape. Syst Biol 49:740–753.

Rohlf FJ, Marcus LF. 1993. A revolution in morphometrics. Trends Ecol Evol 8:129–132.

Roseman CC. 2004. Detecting interregionally diversifying natural selection on modern human cranial form by using matched molecular and morphometric data. Proc Natl Acad Sci USA 101:12824–12829.

Shea BT. 1977. Eskimo craniofacial morphology, cold stress and maxillary sinus. Am J Phys Anthropol 47:289–300.

Slice DE. 1996. Three-dimensional generalized resistance fitting and the comparison of least squares and resistant fit residuals. In: Marcus LF, Corti M, Loy A, Naylor GJP, Slice DE, editors. Advances in morphometrics. NATO ASI Series. New York: Plenum Press. p 179–199.

St. Hoyme LE, Iscan MY. 1989. Determination of sex and race: accuracy and assumptions. In: Iscan MY, Kennedy KAR, editors. Reconstruction of life from the skeleton. New York: Alan R. Liss Inc. p 53–93.

Thomas A, Buxton LHD. 1923. Man's nasal index in relation to certain climatic conditions. J R Anthropol Inst 53:92–122.

Uliyanov YP. 1998. Clinical manifestations of the variants of nasal aerodynamics. Otolaryngol Head Neck Surg 152: 152–153. Available at: http://www.airsilver.net/ch125.html (accessed August 2010).

van Oldenborgh GJ, Balmaseda MA, Ferranti L, Stockdale TN, and Anderson DLT. 2005. Evaluation of atmospheric fields from the ECMWF seasonal forecasts over a 15 year period. J Climate 18:3250–3269.

Weiner JS. 1954. Nose shape and climate. Am J Phys Anthropol 12:615–618.

Yokley TR. 2009. Ecogeographic variation in human nasal passages. Am J Phys Anthropol 138:11–22.